SHELL-MODEL RESULTS IN fp AND $fpg_{9/2}$ SPACES FOR ^{61,63,65}Co ISOTOPES

P.C. Srivastava$^{1,\,*}$ **and V.K.B. Kota**$^{1,\,**}$

^{1}Physical Research Laboratory, Ahmedabad, India

Low-lying spectra and several high-spin states of odd–even ^{61,63,65}Co isotopes are calculated in two different shell-model spaces. First set of calculations have been carried out in fp shell valence space (full fp space for ^{63,65}Co and a truncated one for ^{61}Co) using two recently derived fp shell interactions, namely GXPF1A and KB3G, with ^{40}Ca as core. Similarly, the second set of calculations have been performed in $fpg_{9/2}$ valence space using an fpg effective interaction due to Sorlin *et al.*, with ^{48}Ca as core and imposing a truncation. It is seen that the results of GXPF1A and KB3G are reasonable for ^{61,63}Co. For ^{65}Co, shell-model results show that the fpg interaction adopted in the study is inadequate and also point out that it is necessary to include orbitals higher than $1g_{9/2}$ for neutron-rich Co isotopes.

1. INTRODUCTION

There are many experimental efforts in the recent years to study nuclei around the doubly magic nucleus ^{68}Ni. For example, Lunardi *et al.* have recently populated neutron-rich Fe isotopes from $A = 61$–66, through multi-neutron transfer reactions at Legnaro National Laboratories by coupling the clover detector of Euroball (CLARA) to a PRISMA magnetic spectrometer [1]. The yrast levels of odd–even $^{57-60}$Mn isotopes through multi-nucleon transfer reactions have been reported by Valiente-Dobón *et al.* [2]. More recently Steppenbeck *et al.* [3] have populated high-spin structures in neutron-rich $^{57-60}$Mn isotopes with fusion–evaporation reactions induced by ^{48}Ca beams at 130 MeV on ^{13,14}C targets at

Argonne National Laboratory. Also for many low-lying levels tentative J^π assignments have been made in [3]. Sorlin *et al.* [4] have populated ^{66,68}Ni at GANIL and they proposed evidence for a possible $N = 40$ shell gap. In [5] it is reported that the evolution of shell structure in ^{75}Cu isotopes is due to the inversion of proton $2p_{3/2}$ and $1f_{5/2}$ levels. In another experiment, isomeric low-lying states have been investigated in ^{75}Cu [6]. Using Coulomb excitation of neutron-rich Zn isotopes, for the first time, observation of the 2^+ state in ^{80}Zn has been reported in [7]. Theoretically, importance of the intruder $1g_{9/2}$ orbital for lower fp shell nuclei, namely neutron-rich Cr, Mn, and Fe isotopes, is recently reported in the literature [1, 2, 8–12]. In addition there is growing experimental evidence for collective behavior of Cr and Fe isotopes with $N \sim 40$ and these results suggest that inclusion of both $1g_{9/2}$ and $2d_{5/2}$ orbitals is important for these nuclei [13–15]. In the present paper we consider neutron-rich odd Co isotopes.

Experimental information around and beyond $N = 40$ for Co isotopes is still limited. Recently energy levels of odd–even ^{61,63,65,67}Co isotopes have been reported in the literature. Yrast γ-ray spectroscopy of neutron rich ^{61,63}Co isotopes has been studied by Regan *et al.* [16]. They have observed a rapid decrease in observed energy of the yrast $19/2$ state and yrare $17/2$ state in ^{63}Co compared to ^{59}Co and ^{61}Co, possibly giving an indication of the influence of the neutron $g_{9/2}$ orbital. The level scheme of ^{65}Co has been reported for the first time by Gaudefroy [17]. Similarly, Pauwels *et al.* [18, 19] have investigated the structure of ^{65,67}Co through ^{65,67}Fe β decay and ^{64}Ni$+^{238}$U deep-inelastic reaction. They have suggested a spherical $7/2^-$ ground state and also identified the low-lying $1/2^-$ and $3/2^-$ states in these nuclei. Finally, let us add that Sorlin *et al.* produced $^{67-70}$Co at GANIL [20] and the half-lives for $^{66-71,73}$Co isotopes have been reported [21–24]. In the shell-model (SM) framework, calculations for ^{61,63}Co isotopes have been carried out by Regan *et al.* [16] using fp valence space with ^{48}Ca core and protons occupying only the $f_{7/2}$ orbit. In this truncated fp space they have used a fp shell interaction developed by van Heese and Glaudemans [25]. However, there are not yet any shell-model studies for ^{65,67}Co isotopes. Following our recent SM studies for neutron-rich even–even and odd-A isotopes of Fe [9, 10], odd–odd isotopes of Mn [11], and even–even Ni and Zn and odd-A Cu isotopes [26], in the present paper, we report large shell-model calculations for ^{61,63,65}Co isotopes in extended model spaces: (i) full fp space for ^{63,65}Co and a truncated fp space for ^{61}Co; (ii) $fpg_{9/2}$ space with a truncation for all isotopes. The aim of this study is to analyze the recent experimental data on neutron-rich

Co isotopes and test the suitability of the chosen valence spaces and the effective interactions for these isotopes. We have also made calculations for ^{67}Co and the results are discussed briefly at the end of the paper. Now we will give a preview.

Section 2 gives details of the SM calculations. Sections 3.1–3.3 give the results for odd ^{61}Co, ^{63}Co, and ^{65}Co isotopes, respectively. Finally, Section 4 gives conclusions.

2.   DETAILS OF SHELL-MODEL CALCULATIONS

Odd–even ^{61,63,65}Co isotopes are associated with two shell closures: $Z = 20$, $N = 20$ and $Z = 20$, $N = 28$. In view of this, we have performed two sets of calculations. In the first set, valence space is of full fp shell consisting of $1f_{7/2}$, $2p_{3/2}$, $1f_{5/2}$, $2p_{1/2}$ orbitals for protons and neutrons and treating ^{40}Ca as the inert core. Dimensions of the matrices for ^{61,63,65}Co isotopes in the m-scheme for fp space are shown in Table 1. In the table dimensions for ^{67}Co are also given, as we will discuss the SM results for this isotope briefly at the end of the paper. The dimensions for some J values are as large as $\sim 20 \times 10^6$ and higher. Note that for ^{61}Co a truncation, allowing maximum of four particles (protons plus neutrons) to be excited from $f_{7/2}$ to the remaining three fp orbitals, is used in order to make the calculations tractable. However, the space chosen here is much larger than that used in the previous shell-model study [16]. The fp space calculations are carried out using the recently derived GXPF1A and KB3G interactions. The GXPF1 interaction has been obtained starting from a G-matrix interaction based on the Bonn-C nucleon–nucleon interaction [27] and then modifying the two-body matrix elements by an iterative fitting calculation to about 700 experimental energy levels in the mass range $A = 47$–66 [28]. This interaction predicts a N=34 subshell gap in ^{54}Ca and ^{56}Ti. However, this shell closure was not observed in the experimental studies of the ^{52,54,56}Ti isotopes [29, 30]. This discrepancy led to the modification of the GXPF1 interaction where five T=1 two-body matrix elements, mainly involving the $2p_{1/2}$ and $1f_{5/2}$ orbitals, are adjusted. This modified interaction is referred as GXPF1A [31]. Similarly, the KB3G interaction is extracted from the KB3 interaction by introducing mass dependence and refining its original monopole changes in order to treat properly the $N = Z = 28$ shell closure and its surroundings [32]. Single-particle energies for GXPF1A and KB3G interactions are given in Table 2.

Second set of calculations have been performed in $fpg_{9/2}$ valence space taking ^{48}Ca as the

inert core. The $fpg_{9/2}$ model space comprises of the fp ($1f_{7/2}$, $2p_{3/2}$, $1f_{5/2}$, $2p_{1/2}$) proton orbitals and rg ($2p_{3/2}$, $1f_{5/2}$, $2p_{1/2}$, $1g_{9/2}$) neutron orbitals (with eight $1f_{7/2}$ frozen neutrons). As here the dimensions of the matrices become very large, a truncation has been imposed. We used a truncation by allowing up to a total of four particle excitations from the $1f_{7/2}$ orbital to the upper fp orbitals for protons and from the upper fp orbitals to the $1g_{9/2}$ orbital for neutrons. Dimensions of the matrices for ^{61,63,65,67}Co isotopes in the m-scheme for $fpg_{9/2}$ space are shown in Table 1. The dimensions for some J values are as large as $\sim 10 \times 10^6$ and higher. For the $fpg_{9/2}$ space, with ^{48}Ca core, an interaction reported by Sorlin *et al.* in [4] has been employed. This interaction, called fpg interaction, was built using fp two-body matrix elements (TBME) from [32] and rg TBME from [33]. For the common active orbitals in these subspaces, matrix elements were taken from [33]. As the latter interaction (rg) was defined for a ^{56}Ni core, a scaling factor of $A^{-1/3}$ was applied to take into account the change of radius between the ^{40}Ca and ^{56}Ni cores. The remaining $f_{7/2}g_{9/2}$ TBME are taken from [34]. Single-particle energies for the fpg interaction are given in Table 2.

All the SM calculations have been carried out using the code `ANTOINE` [35, 36] and in this code the problem of giant matrices is solved by splitting the valence space into two parts, one for the protons and the other for the neutrons. The calculations are performed on the 20-node cluster computer at PRL and the computing time, for example, for ^{65}Co is ~ 8 days and ~ 3 days for fp and $fpg_{9/2}$ spaces, respectively.

3.   RESULTS AND DISCUSSION

3.1. ^{61}Co

Ground-state spin and parity $7/2^-$ has been assigned for ^{61}Co following the β decay of ^{61}Fe [37]. Mateja *et al.* [38] have identified $9/2^-$ and $11/2^-$ states at excitation energies of 1285 keV and 1664 keV, using ^{64}Ni($p,\alpha)^{61}$Co reaction. Regan *et al.* [16], using the reaction ^{16}O(^{48}Ca,$p2n)^{61}$Co at a bombarding energy of 110 MeV, were able to confirm the previously assigned $9/2^-$ and $11/2^-$ states at 1285 keV and 1664 keV, respectively [38], and also suggested $1/2^-$ assignment for the 1325-keV level, which is consistent with the earlier assignment [39]. The spins and parities of high-spin low-energy levels have been assigned from angular distributions in reactions and ^{61}Fe β decay [16, 38].

In Fig. 1, experimental data are compared with the calculated energy levels obtained using SM with the three different interactions mentioned before. The calculations predict many more levels than that are observed experimentally below 5 MeV, but we have shown separately only the yrast and yrare levels that correspond to experimental data (we have not shown the low-lying 1/2 and 3/2 levels and they are discussed later). All the interactions predict correct ground-state spin $7/2^-$. The yrast $9/2^-$ state is predicted at 1405 keV by GXPF1A, 1426 keV by KB3G, and fpg interaction as compared to the experimental value 1285 keV. The GXPF1A and KB3G predict the yrast $11/2^-$ above the $9/2^-$ level and the fpg interaction predict $11/2^-$ level below the $9/2^-$ level. In general the agreement between data and the results from GXPF1A and KB3G is reasonable for low-lying levels, as seen from Fig. 1. In [16] levels with spins (tentative) 3/2 and 1/2 are identified at 1028 keV and 1326 keV, respectively. The calculated excitation energy of the first $3/2^-$ level is 804 keV for GXPF1A, 1242 keV for KB3G, and 745 keV for fpg interactions. Similarly the energies for the first $1/2^-$ level are 1295 keV, 1670 keV, and 1173 keV, respectively. Therefore the observed levels at 1028 keV and 1326 keV could be $3/2^-$ and $1/2^-$ levels predicted by the shell-model. In addition, experimental high-spin states with $J > 9/2$ look more like rotational with nearly regular spacing between levels with J and $J - 1$, while calculations show some irregularity. This shows that $1g_{9/2}$ orbital is important in ^{61}Co at high spins.

Table 3 gives information about wave function structure for yrast and few other levels in ^{61}Co (and also for ^{63,65}Co). In this table we have tabulated (i) S, sum of the contributions (intensities) from particle partitions having contribution greater than 1%; (ii) M, the maximum contribution from a single partition; and (iii) N, the total number of partitions contributing to S. The deviation of S from 100% is due to high configuration mixing. The increase in N is also a signature of larger configuration mixing. From the table one can see that for ^{61}Co, S varies from $\sim 72\%$ to $\sim 82\%$; the number of partitions N changing from 13 to 18 and M has variation from $\sim 9\%$ to $\sim 47\%$. For the ground state $7/2^-$ predicted by GXPF1A and KB3G interactions, the partition $\pi(0f_{7/2}^{-1}) \otimes \nu(0f_{7/2}^8 1p_{3/2}^4 0f_{5/2}^2)$ has intensity 22.5% and 30%, respectively. The calculated B(E2) values are shown in Table 4 for a few transitions and it is seen that the B(E2) value for $13/2_1^-$ to $11/2_1^-$ is quite small compared to all other transitions. However, the B(E2) for $13/2_2^-$ to $11/2_1^-$ is strong [B(E2) is ~ 55 e^{2}fm^4 for the two fp interactions]. It is plausible that due to the truncation adopted in the calculations, there could be a change in the positions of the two $13/2^-$ levels.

3.2. ^{63}Co

Experimentally Runte *et al.* [40] have proposed $7/2^-$ ground state for ^{63}Co from the β^- decay studies of ^{63}Fe. Regan *et al.* [16], using the reaction ^{18}O(^{48}Ca,$p2n$)^{63}Co at a bombarding energy of 110 MeV, strongly suggested $J^\pi = 9/2^-$ for the level at 1383 keV, and similarly $11/2^-$ assignment for the level at 1673 keV has been proposed. In Fig. 2 the calculated energy levels obtained using SM are compared with experimental data [16]. All the three interactions predict correct ground-state spin. The calculated excitation energy for the $9/2_1^-$ is 1154 keV for GXPF1A, 1301 keV for KB3G, and 1607 keV for fpg interaction. Experimentally only one $9/2^-$ state is observed, but theoretically a second $9/2^-$ is predicted at about 1 MeV higher than the first one by all the interactions (these are not shown in the figure). The first yrast $3/2^-$ state is predicted by GXPF1A and fpg interactions at $\sim$ 100 and $\sim$ 200 keV below the experimental value of 995 keV, while KB3G predicts this level at $\sim$ 300 keV higher. Similarly, the first $11/2^-$ state is predicted at 1535 keV by GXPF1A, 1747 keV by KB3G, and 1418 keV by fpg interaction and the corresponding experimental value is 1673 keV.

From Table 3 one can see that for ^{63}Co, there are 9–17 partitions giving a total of $\sim$ 77–85% of the total intensity and the maximum intensity from a single partition is $\sim$ 16–45%. For the $7/2^-$ ground state the partition $\pi(0f_{7/2}^{-1}) \otimes \nu(0f_{7/2}^8 1p_{3/2}^4 0f_{5/2}^4)$ has intensity 31.8% and 44.8%, respectively, for GXPF1A and KB3G interactions. Table 4 gives the calculated B(E2) values for a few transitions. The B(E2) values confirm that the ground state $7/2^-$ and the $9/2^-$ (1383 keV) and $11/2^-$ (2539 keV) levels form a band-like structure. The $11/2^-$ at 1673 keV belongs to a different structure, consistent with the claim by Regan *et al.* [16]. The ^{61}Co and ^{63}Co results in Figs. 1 and 2 establish that the fp space is adequate up to about $\sim$ 3 MeV excitation for these nuclei, but the interactions GXPF1A and KB3G require some modifications for producing much better agreements with experimental data. Alternatively, as the fpg interaction results do not show much improvement over the fp results, a better $fpg_{9/2}$ interaction may improve the results.

3.3. ^{65}Co

In Fig. 3, the calculated energy levels for ^{65}Co obtained using SM with the three different interactions together with the experimental data [19] are shown. All the interactions predict

correct ground-state spin as observed in experiment. The experimental energy of the first $9/2^-$ level is 1479 keV, while the calculated values are 1753 keV for GXPF1A, 1943 keV for KB3G, and 2042 keV for fpg interaction. Similarly, the first $3/2^-$ state is predicted to be too low by GXPF1A and KB3G and at about 250 keV higher by fpg interaction (experimental value is 883 keV). Above 2 MeV, the order of $11/2^-$, $13/2^-$, and $15/2^-$ is seen in experimental data is different from the order given by GXPF1A and KB3G interactions. However, the fpg interaction gives $11/2^-$ as lowest and then nearly degenerate $13/2^-$ and $15/2^-$ levels. Lowest $3/2^-$ and $11/2^-$ are much lower for GXPF1A and KB3G interactions and their positions are better predicted by the fpg interaction. Combining all these, we conclude that for ^{65}Co, fpg interaction gives better results. However the energies predicted by the fpg interaction show that modifications of this interaction are clearly needed.

Table 3 gives some information about wave function structure as generated by the fpg interaction for ^{65}Co. It is seen that ~ 11–18 partitions generate ~ 81–84% of the intensity. The calculated B(E2) values for fpg interaction for $9/2_1^- \rightarrow 7/2_1^-$, $11/2_1^- \rightarrow 9/2_1^-$, $11/2_2^- \rightarrow 9/2_1^-$ transitions are 105.12, 0.28, and 1.29 e^2fm^4, respectively. Thus, there is a change of structure after $9/2^-$ with $g_{9/2}$ occupancy for neutrons becoming large. For $11/2_1^-$ the occupancy is ~ 0.8 and for $11/2_2^-$ it is ~ 1.5. Similarly, wave functions show that the $11/2_1^-$ states contain partitions with $g_{9/2}$ orbital contributing to ~ 40–60% of the intensity.

For further tests of the adopted fpg interaction, we have made SM calculations also for ^{67}Co. Its ground-state spin $7/2^-$ is correctly predicted by the SM calculations. Pauwels *et al.* [18] have identified $(1/2^-)$ isomeric state in ^{67}Co with a half-life of 496(33) ms at an unexpected low energy of 492 keV. It is claimed [41] that strong proton–neutron correlations inducing deformation are responsible for the decrease in excitation energy of the $1/2^-$ state. Firstly, the position of the first $1/2^-$ and $3/2^-$ (680 keV) levels are predicted to be at very high excitation (> 4 MeV) compared to data by GXPF1A and KB3G interactions. Thus clearly fp space is not adequate for this nucleus. The SM calculations with fpg interaction gave the first $1/2^-$, $3/2^-$, and $5/2^-$ at 2118 keV, 1157 keV, and 1728 keV, respectively, while the data values are 492 keV, 680 keV, and 1252 keV. Thus, for a good description of the spectra of neutron-rich Co isotopes, the fpg interaction adopted in the present study clearly needs modifications. Towards this end we have made calculations for ^{65}Co using various monopole corrections [42].

A significant decrease of the energy gap between proton $1f_{7/2}$ and $1f_{5/2}$ orbitals is obtained

for the fpg interaction with the increase of the occupation of the $\nu g_{9/2}$ orbital, usually referred to as monopole migration. Otsuka *et al.* in [43] have shown that this is due to opposite actions of the strong proton–neutron tensor force on the $\pi f_{7/2}$ and $\pi f_{5/2}$ orbitals while filling the neutrons in the $1g_{9/2}$ orbital. To study the importance of the monopole corrections to the fpg interaction, we have modified the $1g_{9/2}1f_{7/2}$ matrix elements by subtracting 100 keV and $g_{9/2}f_{5/2}$ matrix elements by adding 100 keV, so that the $1f_{7/2}$–$1f_{5/2}$ proton gap is increased for neutron-rich nuclei. With this modified interaction, the $3/2_1^-$, $11/2_1^-$, $9/2_1^-$, and $1/2_1^-$ levels in ^{65}Co are predicted at 740, 1115, 1584, and 1880 keV, respectively. The $1/2_1^-$ level is still predicted at much higher energy than the experimental value and also the $11/2_1^-$ level is too low. Calculations are also performed by changing the original matrix elements by 200 keV and found no significant improvement in the results. In addition, calculations are also carried out by modifying $p_{1/2}g_{9/2}$ matrix elements (by $50 - 200$ keV) and also $p_{3/2}g_{9/2}$ matrix elements (by 100 keV). Again, not much improvement is seen in the above results. All these results clearly show that one has to go beyond $fpg_{9/2}$ space and include higher orbitals.

4. CONCLUSIONS

In the present work, the results of large scale shell-model calculations are reported for neutron-rich odd–even isotopes of Co with $A = 61$, 63, and 65 in two valence spaces: full fp space and $fpg_{9/2}$ space with ^{48}Ca core. For ^{61}Co a truncation has been adopted, but the matrix dimensions for the present calculations are larger than the previous fp calculations. On the other hand, full fp space results with the recently derived GXPF1A and KB3G interactions are reported for ^{63,65}Co. Similarly, for the $fpg_{9/2}$ space calculations, a truncation has been adopted and the so-called a fpg interaction is employed. Results for energy spectra shown in Figs. 1 and 2 for ^{61,63}Co confirm (see also the discussion in Sections 3.1 and 3.2) that the fp space results with GXPF1A and KB3G are reasonable when compared with data (note that in [16] shell-model results are presented only in a restricted fp space and also with a special effective interaction). For ^{65}Co the results in the extended model space, i.e., in $fpg_{9/2}$ space do not reproduce correct experimental findings, and further, with monopole correction by reducing the gap between $f_{7/2}$–$f_{5/2}$, the $1/2_1^-$ is still high and $11/2_1^-$ is low. Thus it appears to be necessary to include the intruder $2d_{5/2}$ orbital while approaching $N \sim 40$.

In the last decade good fp space effective interactions, with ^{40}Ca core, have been generated giving good SM spectroscopy [42]. Recently, a good effective interaction (JUN45) in $f_{5/2}pg_{9/2}$ space, with ^{56}Ni core, has been reported with an extensive set of SM calculations by Honma et $al.$ [44]. In addition, the so-called fpg interaction in $fpg_{9/2}$ space with ^{48}Ca core has some limited success [4, 11]. However, combining the results of the present paper with our previous large shell-model studies of neutron-rich Fe and Mn isotopes [9–11], we conclude that it is necessary to generate good $fpg_{9/2}$ and $fpg_{9/2}d_{5/2}$ space effective interactions (with ^{48}Ca core) for neutron-rich Fe, Mn, and Co isotopes. After the present work was complete, there appeared a report giving some results for low-lying yrast levels in even–even Cr and Fe isotopes, showing collective effects as N approached 40, obtained using a new hybrid interaction in $fpg_{9/2}d_{5/2}$ space [45]. It remains to be seen if this interaction can describe (here matrix dimensions will be $\sim 10^{10}$ and higher) the experimental data on neutron-rich odd Co isotopes.

---

1. S. Lunardi et $al.$, Phys. Rev. C **76**, 034303 (2007).

2. J. J. Valiente-Dobón et $al.$, Phys. Rev. C **78**, 024302 (2008).

3. D. Steppenbeck et $al.$, Phys. Rev. C **81**, 014305 (2010).

4. O. Sorlin et $al.$, Phys. Rev. Lett. **88**, 092501 (2002).

5. K. T. Flanagan et $al.$, Phys. Rev. Lett. **103**, 142501 (2009).

6. J. M. Daugas et $al.$, Phys. Rev. C **81**, 034304 (2010).

7. J. Van de Walle et $al.$, Phys. Rev. Lett. **99**, 142501 (2007).

8. K. Kaneko, Y. Sun, M. Hasegawa, and T. Mizusaki, Phys. Rev. C **78**, 064312 (2008).

9. P. C. Srivastava and I. Mehrotra, J. Phys. G **36**, 105106 (2009).

10. P. C. Srivastava and I. Mehrotra, Phys. Atom. Nucl. **73**, 1656 (2010).

11. P. C. Srivastava and I. Mehrotra, Eur. Phys. J. A **45**, 185 (2010).

12. Y. Sun, Y.-C. Yang, H.-L. Liu, K. Kaneko, M. Hasegawa, and T. Mizusaki, Phys. Rev. C **80**,

054306 (2009).

13. N. Aoi *et al.*, Phys. Rev. Lett. **102**, 012502 (2009).

14. A. Gade *et al.*, Phys. Rev. C **81**, 051304(R) (2010).

15. J. Ljungvall *et al.*, Phys. Rev. C **81**, 061301(R) (2010).

16. P. H. Regan, J. W. Arrison, U. J. Hüttmeier, and D.P. Balamuth, Phys. Rev. C **54**, 1084 (1996).

17. L. Gaudefroy, Ph.D. Thesis, Université de Paris XI, Orsay (2005).

18. D. Pauwels *et al.*, Phys. Rev. C **78**, 041307(R) (2008).

19. D. Pauwels *et al.*, Phys. Rev. C **79**, 044309 (2009).

20. O. Sorlin *et al.*, Nucl. Phys. A **669**, 351 (2000).

21. W. F. Mueller *et al.*, Phys. Rev. Lett. **83**, 3613 (1999).

22. L. Weissman *et al.*, Phys. Rev. C **59**, 2004 (1999).

23. W. F. Mueller *et al.*, Phys. Rev. C **61**, 054308 (2000).

24. M. Sawicka *et al.*, Eur. Phys. J. A **22**, 455 (2004).

25. A. G. M. van Heese and P. W. M. Glaudemans, Z. Phys. A **303**, 267 (1981).

26. P. C. Srivastava, Ph.D. Thesis, University of Allahabad (Allahabad, India, 2010).

27. M. Hjorth-Jensen, T.T.S. Kuo, and E. Osnes, Phys. Rept. **261**, 125 (1995).

28. M. Honma, T. Otsuka, B. A. Brown, and T. Mizusaki, Phys. Rev. C **65**, 061301(R) (2002).

29. D. -C. Dinca *et al.*, Phys. Rev. C **71**, 041302(R) (2005).

30. B. Fornal *et al.*, Phys. Rev. C **70**, 064304 (2004).

31. M. Honma,T. Otsuka, B.A. Brown, and T. Mizusaki, Eur. Phys. J. A **25**, 499 (2005).

32. A. Poves, J. Sanchez- Solano, E. Caurier, and F. Nowacki, Nucl. Phys. A **694**, 157 (2001).

33. F. Nowacki, Ph.D. Thesis (IRes, Strasbourg, 1996).

34. S. Kahana, H.C. Lee, and C.K. Scott, Phys. Rev. **180**, 956 (1969).

35. E. Caurier, code ANTOINE (Strasbourg, 1989), unpublished.

36. E. Caurier and F. Nowacki, Acta Phys. Pol. B **30**, 705 (1999).

37. J. Bron, H.W. Jongsma, and H. Verhul, Phys. Rev. C **11**, 996 (1975).

38. J.F. Mateja *et al.*, Phys. Rev. C **13**, 2269 (1976).

39. K.L. Coop, I.G. Graham, and E. Titterton, Nucl. Phys. A **150**, 346 (1970).

40. E. Runte *et al.*, Nucl. Phys. A **441**, 237 (1985).

41. K. Heyde, P. Van Isacker, M. Waroquier, J.L. Wood, and R.A. Mayer, Phys. Rept. **102**, 291 (1983).

42. E. Caurier, G. Martinez-Pinedo, F. Nowacki, A. Poves, and A.P. Zuker, Rev. Mod. Phys. **77**, 427 (2005).

43. T. Otsuka, T. Matsuo, and D. Abe, Phys. Rev. Lett. **97**, 162501 (2006).

44. M. Honma, T. Otsuka, T. Mizusaki, and M. Hjorth-Jensen, Phys. Rev. C **80**, 064323 (2009).

45. S.M. Lenzi, F. Nowacki, A. Poves, and K. Sieja, Phys. Rev. C **82**, 054301 (2010).

Table 1. Dimensions of the shell-model matrices for ^{61,63,65,67}Co in the m-scheme for fp and $fpg_{9/2}$ spaces. The fp space dimensions given in the table for ^{63}Co, ^{65}Co and ^{67}Co are for the full fp space. However, for ^{61}Co, the dimensions are given for the truncated fp space with maximum of four particles excited from $1f_{7/2}$ orbital to the rest of the fp orbitals. For $fpg_{9/2}$ space, the dimensions are for the truncation explained in the text.

Table 2. Single-particle energies (in MeV) for GXPF1A, KB3G, and fpg interactions.

Table 3. The extent of configuration mixing involved in ^{61,63,65}Co isotopes for different states (for each state the numbers quoted are S, sum of the contributions from particle partitions, each of which is contributing greater than 1%; M, maximum contribution from a single partition; and N, total number of partitions contributing to S). Note that S and M are in percentage.

Table 4. Calculated B(E2) values for some transition for ^{61,63}Co isotopes with standard effective charges: e^{π}_{eff}=1.5e, e^{ν}_{eff}=0.5e. All B(E2) values are in e^2fm^4 unit (the experimental γ-ray energies corresponding to these transitions are also shown).

Fig. 1. Experimental data [16] for ^{61}Co compared with shell-model results generated by three different effective interactions. See text for details.

Fig. 2. The same as in Fig.1, but for ^{63}Co.

Fig. 3. The same as in Fig.1, but for ^{65}Co.

Table 1. Dimensions of the shell-model matrices for ^{61,63,65,67}Co in the m-scheme for fp and $fpg_{9/2}$ spaces. The fp space dimensions given in the table for ^{63}Co, ^{65}Co and ^{67}Co are for the full fp space. However, for ^{61}Co, the dimensions are given for the truncated fp space with maximum of four particles excited from $1f_{7/2}$ orbital to the rest of the fp orbitals. For $fpg_{9/2}$ space, the dimensions are for the truncation explained in the text.

	fp space(^{40}Ca core)				$fpg_{9/2}$ space(^{48}Ca core)			
$2J^{\pi}$	^{61}Co	^{63}Co	^{65}Co	^{67}Co	^{61}Co	^{63}Co	^{65}Co	^{67}Co
1^-	17034417	28464525	1227767	7531	9480566	12957305	6308001	874872
3^-	16458582	27480719	1176872	7116	9188151	12599047	6139881	850942
5^-	15361866	25609431	1080985	6352	8629526	11911108	5816312	804889
7^-	13846120	23028746	950895	5347	7853482	10947190	5361260	740166
9^-	12044787	19971189	800263	4226	6924099	9778867	4806873	661360
11^-	10105027	16691144	643552	3135	5912846	8487672	4190319	573863
13^-	8167820	13430682	493609	2161	4888828	7155066	3549245	483060
15^-	6353114	10392710	360351	1378	3912382	5855328	2918851	394088
17^-	4747943	7721925	249638	801	3028771	4648184	2328191	311094
19^-	3403216	5499474	163574	421	2267035	3576504	1799122	237276

Table 2. Single-particle energies (in MeV) for GXPF1A, KB3G, and fpg interactions.

Orbital	GXPF1A	KB3G	fpg
$1f_{7/2}$	-8.6240	0.0000	0.000
$2p_{3/2}$	-5.6793	2.0000	2.000
$2p_{1/2}$	-4.1370	4.0000	4.000
$1f_{5/2}$	-1.3829	6.5000	6.500
$1g_{9/2}$	-	-	9.000

Table 3. The extent of configuration mixing involved in ^{61,63,65}Co isotopes for different states (for each state the numbers quoted are S, sum of the contributions from particle partitions, each of which is contributing greater than 1%; M, maximum contribution from a single partition; and N, total number of partitions contributing to S). Note that S and M are in percentage.

J^π	$^{63}_{27}$Co$_{36}$			J^π	$^{65}_{27}$Co$_{38}$			J^π	$^{65}_{27}$Co$_{38}$		
	S	M	N		S	M	N		S	M	N
	GXPF1A				GXPF1A				fpg		
$7/2^-_1$	71.6	22.5	18	$7/2^-_1$	80.7	31.8	14	$7/2^-_1$	83.0	47.9	11
$3/2^-_1$	63.4	9.0	18	$3/2^-_1$	76.8	16.1	15	$3/2^-_1$	81.1	27.2	16
$9/2^-_1$	71.9	16.2	17	$9/2^-_1$	85.1	34.1	17	$9/2^-_1$	84.3	42.9	16
$11/2^-_1$	67.4	15.5	17	$11/2^-_1$	80.8	28.6	15	$11/2^-_1$	83.0	26.9	17
$13/2^-_1$	74.4	35.0	12	$11/2^-_2$	80.7	30.2	14	$11/2^-_2$	78.1	12.1	18
$13/2^-_2$	75.5	30.7	15	$13/2^-_2$	81.6	30.5	13				
	KB3G				KB3G						
$7/2^-_1$	76.6	30.0	18	$7/2^-_1$	82.9	44.8	12				
$3/2^-_1$	71.1	20.8	14	$3/2^-_1$	82.9	30.3	15				
$9/2^-_1$	75.5	13.0	16	$9/2^-_1$	81.9	31.6	11				
$11/2^-_1$	76.3	27.4	17	$11/2^-_1$	81.1	35.7	11				
$13/2^-_1$	82.0	47.5	13	$11/2^-_2$	83.1	32.8	11				
$13/2^-_2$	79.8	37.7	15	$13/2^-_2$	82.5	35.8	9				

Table 4. Calculated B(E2) values for some transition for ^{61,63}Co isotopes with standard effective charges: e^{π}_{eff}=1.5e, e^{ν}_{eff}=0.5e. All B(E2) values are in e^2fm^4 unit (the experimental γ-ray energies corresponding to these transitions are also shown).

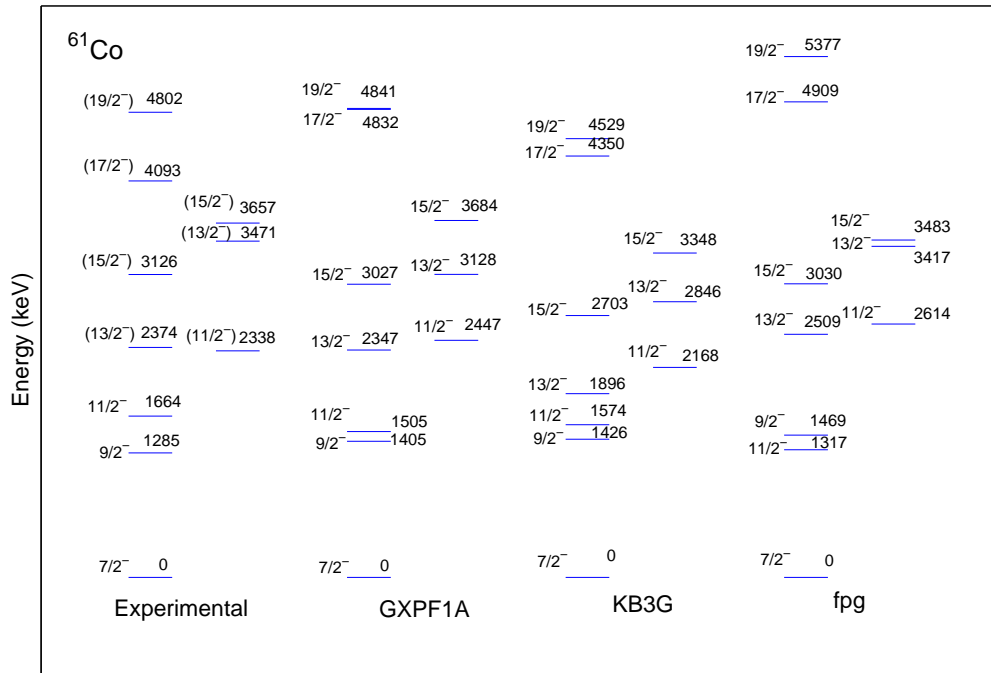| Nucleus	Transition	E_γ, keV	GXPF1A	KB3G
^{61}Co	$B(E2;\ 9/2_1^- \rightarrow 7/2_1^-$)	1285	209.47	132.60
	$B(E2;\ 11/2_1^- \rightarrow 9/2_1^-$)	379	144.61	31.20
	$B(E2;\ 13/2_1^- \rightarrow 11/2_1^-$)	710	8.13	0.54
	$B(E2;\ 15/2_1^- \rightarrow 13/2_1^-$)	752	31.18	65.50
^{63}Co	$B(E2;\ 9/2_1^- \rightarrow 7/2_1^-$)	1383	164.55	131.84
	$B(E2;\ 11/2_2^- \rightarrow 9/2_1^-$)	1156	157.78	120.35
	$B(E2;\ 11/2_1^- \rightarrow 9/2_1^-$)	290	2.04	2.92
	$B(E2;\ 13/2_1^- \rightarrow 11/2_1^-$)	495	42.44	60.50

Figure 1. Experimental data [16] for ^{61}Co compared with shell-model results generated by three different effective interactions. See text for details.
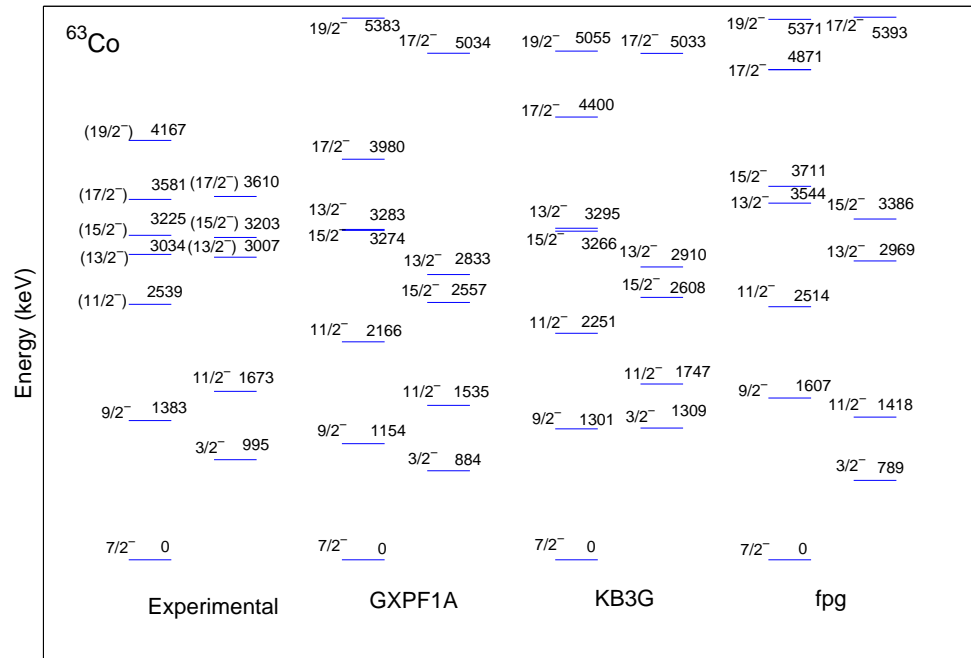
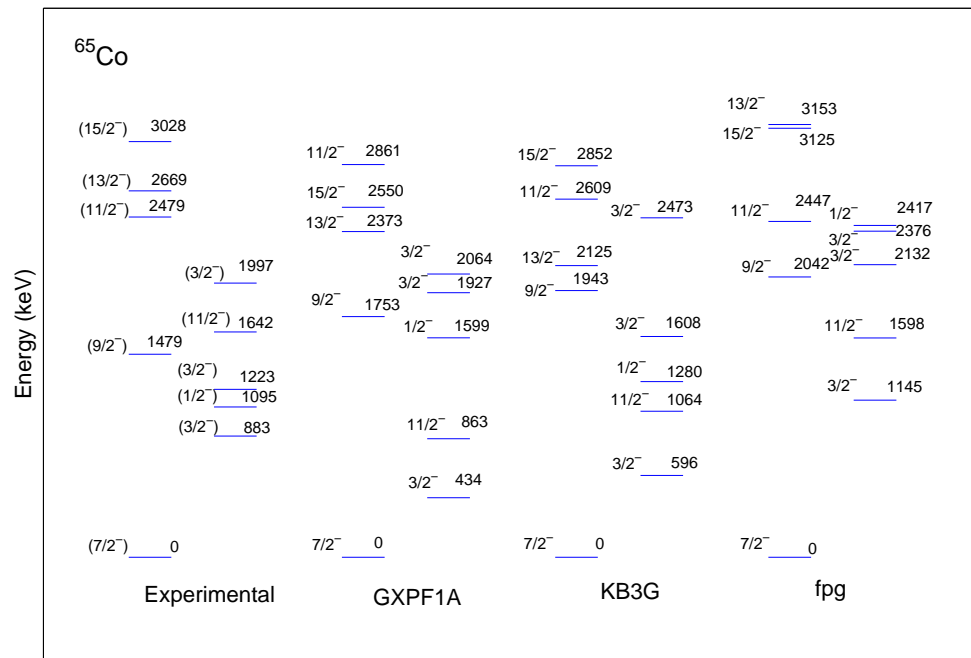**Figure 2.** The same as in Fig.1, but for ^{63}Co.

Figure 3. The same as in Fig.1, but for ^{65}Co.